



SYNTHESIS AND CHARACTERIZATION OF LETROZOLE-LOADED POLYMER BASED NANOPARTICULATE FORMULATIONS

1077

SANDHYA RANI MANDADI^{A, B*}, LANKALAPALLI SRINIVAS^A

^aDepartment of Pharmaceutics, GITAM Institute of Pharmacy GITAM (Deemed University) University, Rushikonda, Visakhapatnam - 530045, Andhra Pradesh, India.

^bCentre for Molecular Cancer Research (CMCR), Vishnu Institute of Pharmaceutical Education and Research, Narsapur-

Corresponding Author: Ms. Sandhya Rani Mandadi, Centre for Molecular Cancer Research (CMCR),

Vishnu Institute of Pharmaceutical Education and Research,

Narsapur-502313, Telangana, India,

Email: sandhyareddy.m@viper.ac.in

ABSTRACT

Breast cancer (BC) is one of the most commonly diagnosed malignancies in the world. It is responsible for the majority of female mortality. Letrozole (LTZ) is an effective treatment for postmenopausal women whose BC responds positively to hormone receptors, but it has also been reported to have some unpleasant side effects. The inherent limitations of current anticancer drugs require the development of innovative technologies for more effective and safer cancer therapy. To address this problem, in this study, we fabricated unique PLGA nanoparticles loaded with LTZ. Optimized LTZ-PLGA nanoparticles (LTZ-PLGA NP) exhibited a particle size of 53.19 nm, with a polydispersity index (PDI) of 0.387 and a negative zeta potential of -10.9 mV. LTZ-PLGA NP also showed dose-dependent cell toxicity against MDA-MB-231 human breast cancer cell lines, with an inhibitory concentration (IC₅₀) of 5.64 ± 0.346 µg/ml. The hemolytic properties indicate that LTZ-PLGA NPs are compatible with blood components. In general, the newly synthesized LTZ-PLGA NPs were in the nanosize range, had good entrapment efficiency and a slow drug release profile with good inhibitory concentrations against MDA-MB-231.

Keywords: Breast cancer; letrozole; nanoparticle; MDA-MB-231

DOI Number: 10.14704/NQ.2022.20.12.NQ77089

NeuroQuantology2022;20(12): 1077-1087

INTRODUCTION

Breast cancer (BC) is the most frequently diagnosed cancer in women and the leading cause of death^{1,2}. The World Health Organization (WHO) reports that approximately six million women developed breast cancer in 2018. It is the third most commonly diagnosed cancer worldwide³. It is estimated to surpass the death rate from heart disease in the coming years⁴.

BC is a very diverse disease in genetic, histopathological, and therapeutic terms⁵. Due to the heterogeneity, complexity, and aggressiveness of BC, treatment of BC represents a significant therapeutic obstacle⁶. The main approaches to treat BC are surgery, chemotherapy, radiation and hormonal therapy, and then targeted therapy^{7,8}. For women with early BC, surgical resection is the gold standard. Chemotherapy and radiation therapy have shown

some promising benefits in the treatment of BC but also have some major side effects. These include collateral damage, which is due to the drug damaging cancer cells, while vital cells may be destroyed due to side effects of treatment that trigger tissue death⁹. Other obstacles to chemotherapy include microenvironmental signals that reduce the effectiveness of the therapeutic agent¹⁰. To address these issues, a novel drug delivery system is required that efficiently targets tumors¹¹. In general, novel nanoparticle-based drug delivery systems (NDDS) have shown promising efficacy in cancer therapy due to their enhanced permeability and retention (EPR)^{12,13}.

To reduce adverse effects and increase efficacy, we need to find a highly efficient and cost-effective treatment approach for BC. In an effort to improve the potential for site-specific delivery of anticancer



drugs to tumors, polymeric core-shell nanoparticles are currently being developed, which are characterized by their ease of use^{14,15}. Among the various delivery systems, polymeric nanoparticles seem to be particularly attractive and promising. This is due to their well-defined morphological structures, size, low polydispersity index, and high transfection efficiency^{16,17}. Despite all these advantages, their drug loading capacity is limited¹⁸⁻¹⁹.

There are a number of therapeutic modalities for the treatment of BC, including letrozole (LTZ), which has limited BC efficacy. It is one of the most effective third-generation triazole aromatase inhibitors (AIs). It is approved by the Food and Drug Administration (FDA) for the treatment of advanced stage BC in postmenopausal women and inhibits the biosynthesis of excess estrogen in the body²⁰. LTZ can be encapsulated in biodegradable NPs for sustained delivery to suppress estrogen production at the receptor site. Biodegradable matrices would slowly dissolve and release the drug.

To date, there are few reports suggesting that polymeric nanoparticles may be a good option for LTZ delivery. Sustained-release LTZ nanoparticles were developed by Gomathi et al. and prepared from chitosan using sodium tripolyphosphate as a cross-linking agent to overcome the drawbacks of low loading efficiency, higher particle size, etc. The way the formulations were made was analyzed and they were tested for effective drug release in vitro, blood compatibility, stability, and biocompatibility. It further meets cancer treatment needs²¹.

In general, the development of new materials always leads to technological progress and creates innovative solutions to old problems. Thus, nanotechnology has gained a broad acceptance in contemporary life. Hence, the present work was aimed at synthesis of the novel formulation and its effectiveness has been evaluated. We prepared letrozole-loaded poly(lactide-co-glycolide) nanoparticles (LTZ-PLGA-NPs) by the emulsion-solvent evaporation technique using dichloromethane (DCM) as organic solvent and polyvinyl alcohol (PVA) as colloid stabilizer to obtain a smaller particle size with high entrapment efficiency and sustained release profile. The particle size,

morphology, entrapment efficiency, drug-polymer interaction, and in vitro release of LTZ-PLGA-NPs were studied. The influence of the percentage of drug (relative to the mass of the polymer) on the performance of the formulation, including particle size, zeta potential, entrapment efficiency, and in vitro release, was investigated. The purpose of this study is to investigate the development of a novel and sustained LTZ delivery system using biodegradable PLGA against MDA-MB-231.

2. MATERIALS AND METHODS

The letrozole powder was provided by Hetero drugs Pvt. Ltd, Hyderabad. Poly (D, L-lactide-co-glycolide), PLGA 75:25 having molecular weight 15000, chloroform, polyvinyl alcohol (PVA): Mw = 89,000–98,000; 99% hydrolyzed, Dichloromethane (DCM), polysorbate 80 (Tween 80) and dialysis bag (MW cutoff = 14 000) were obtained from Sigma-Aldrich Co. LLC. All other chemicals and reagents are analytically graded and used without further modification.

The rabbit blood withdrawal was carried out according to the guidelines of the institutional Animal Ethics Committee, VIPER, Narsapur, Hyderabad, under the approval number (01/IAEC/VIPER/Ph.D/2021-2022).

2.1. Preparation of poly(lactic acid-co-glycolic acid) (PLGA) nanoparticles loaded with LTZ

PLGANP loaded with LTZ was prepared by the solvent evaporation process²². The aqueous phase contains a solution of polyvinyl alcohol (PVA) at a concentration of 2%, while the organic phase consists of PLGA (75:25). LTZ (20 mg) was dissolved in dichloromethane (DCM) containing 25 mg of PLGA. The organic phase solution was slowly poured into 10 ml of a 0.75% aqueous PVA solution under magnetic stirring. The resulting O/W emulsion was sonicated for 90 seconds. The organic mixture was immediately removed by slow stirring at room temperature for 6 hours using a magnetic stirrer. This was to ensure that all of the organic solvent had evaporated. LTZ-PLGA -The nanoparticles were centrifuged at 25,000 rpm (44,800 g) at 5 ° C for further studies.

2.2. Characteristics of the final selected formulation (F5)



2.2.1. Morphology study

Field-emission scanning electron microscopy (FE-SEM) microscopes (Supra 55, Carl Zeiss, Germany) were used to monitor the formation of LTZ-PLGA -NPs. It was equipped with a tungsten filament and provided high-quality images with a small electrical pulse.

The sample was examined for morphology using a transmission electron microscope (TEM) (Tecnai 2, 120 KV, FEI Company, Eindhoven, The Netherlands) after a drop of the sample solution was applied to a 300 mesh carbon coated gold matrix. The solution was dried overnight and after complete drying, the second drop was applied. Again, drying was done overnight.

2.2.3. Estimation of encapsulation efficiency (% EE)

50 mg of air-dried LTZ-PLGA -NPs was kept in 5 mL of phosphate buffered saline (PBS) for 1 hour. It was filtered through a 0.22 µm membrane filter²⁷. Then the stock solution of the formulation was further diluted with PBS. The drug content in the filter was then analyzed using a UV spectrometer at 240 nm. The percentage (%) EE can be calculated using the established equation (i)^{11,28}.

$$\%EE = \frac{(Total\ amount\ of\ LTZ - Amount\ of\ LTZ\ in\ supernatant)}{Total\ amount\ of\ LTZ} \times 100 \dots \dots Eq. (i)$$

2.2.4. In vitro drug release studies

The in vitro release of LTZ from LTZ-PLGA-NP was studied according to the previously published technique¹⁷. The dialysis bag method was used with PBS with a pH of 7.4 and simulated cancer conditions (pH 5.0) for 48 hours each at 37 ° C. The dialysis membrane used has a molecular weight cut-off (MWCO) between 12,000 and 14,000 Da. The sample of 10 mg LTZ-PLGA-NPs was dissolved in 10 ml of distilled water and sealed in a dialysis bag. 50 mL of PBS at pH 7.4 and sodium acetate buffer at pH 5.0 were used to carry out the drug-release study. 3 mL of the samples were removed from the release medium at a fixed time interval and replaced with the same amount of fresh PBS to obtain a standardized volume and sink condition. The amount of LTZ present in the samples was calculated by UV spectrophotometry at 240 nm wavelength. The studies were carried out in triplicate.

2.2.5. In vitro hemolysis assay

Hemolytic tests were used to determine the biocompatibility of nanocarriers. The hemolytic activity of PLGA-NP and LTZ was tested at a dose of 1 mg / ml. Rabbit blood (5 ml) was obtained in a sealed ethylenediaminetetraacetic acid (EDTA) tube and used within one hour. The blood was submerged at 3000 rpm for 10 minutes to separate the red blood cells (RBCs) from the blood sample. Separated RBCs were eroded three times with PBS (7.4) and diluted with 900 µg saline and 1% Triton X-100 as a positive control. 96-well plates containing 100 µl of erythrocyte suspension were treated with different concentrations of nanocarriers. Finally, the plate was gently shaken and incubated at 37 ° C for three hours. The resulting supernatants were examined with a UV-vis spectrophotometer using plate readers at 541 nm. The percentage of hemolysis was measured according to equation (ii). Here, At is the absorbance of the treated supernatant, Ac is the absorbance of the negative control, and Ax is the absorbance of the positive control.

The samples were then analyzed and photographed using TEM at 100 KV²³⁻²⁴.

2.2.2. Particle size analysis and surface charge measurement

The nanoparticle size and Zeta potential of the formulations were determined using the Malvern ZS zetasizer (Malvern Instrument, Worcestershire, United Kingdom). The diameter and polydispersion index (PDI) of the formulation in homogeneous mixtures were determined using the dynamic light dispersion (DLS) technique. The extended levels remained prepared by laser wavelength 633.0 nm at 25 ° C at a 90° revealing angle. The size of the particles was determined with the help of Master Sizer 3000 software²⁵⁻²⁶.



$$\% \text{Hemolysis} = \frac{(At - Ac)}{(Ax - Ac)} \times 100 \dots \dots \text{Eq. (ii)}$$

2.2.6. Cytotoxicity assay

To determine the cytotoxicity of the nanoformulation, a colorimetric assay was performed with 3-[4,5-dimethylthiazol-2-yl] -2,5-diphenyl-2H-tetrazolium (MTT) using the Mosmann technique^{29,30}. MDA-MB -231 breast cancer cell lines were selected for the cytotoxicity study. Basically, 96-well plates containing 5000 cells/wells of MDA-MB -231 were collected. They were allowed to grow for 24 hours. 100 µl of cells were inoculated in 96-well microtiter plates at different densities according to the developmental characteristics of each cell. Incubation was carried out in CO₂ (5%) at 37 ° C for 24 hours. The microtiter plates were removed from the incubator and washed with 200 µl of PBS after the supernatant was removed. Then 200 µl of medium (DMEM for cancer cells) and 30 µl of 5 mg/ml MTT were added. The microtiter plates were incubated at 37 ° C for four hours. After incubation of the cells, the supernatant was separated and 50 µl DMSO was added. A microplate reader was used to calculate the MTT reduction at a wavelength of 540 nm and a reference wavelength of 630 nm. The analysis was performed in triplicate. Data were analyzed using Graph Pad Prism 5.0. and expressed as mean ± standard deviation. IC₅₀ values were analyzed from in vitro dose-response curves using linear regression analysis³¹.

$$\% \text{ Cell viability} = \frac{(A540 \text{ nm treated cells})}{(A540 \text{ nm untreated cells})} \times 100 \dots \dots \text{Eq. (iii)}$$

2.2.7. Stability studies of the final formulation

The stability of the final optimized formulation was evaluated by placing the formulation at room temperature in accordance with the guidelines of the International Conference on Harmonization (ICH, 2003) for one month. The added drug content in the formulation was calculated in regular time gaps (1, 15 and 30 days). Using a UV spectrophotometer, mutations in the uniformity of the final formulation were examined^{32,33}.

3. RESULTS AND DISCUSSION

3.1.1. Morphological analysis

This study was characterized by the incorporation of LTZ-PLGA-NPs with different techniques. Transmission electron microscopes (TEMs) have been used to evaluate the morphology of the surface. The uniform spherical size with a particle size of 50 nm was evident from the TEM assessment. TEM micrographs demonstrating the size of the nanoformulation in the size range below 50 nm, as shown in **Figure 1 (a)**. SEM was used to characterize the shape of LTZ-PLGA-NPs. The SEM image shows the particle structure as in **Figure 1 (b)**, a smooth surface and a thickness of 100 nm. All LTZ-PLGA-NPs were nearly spherical in shape, without significant aggregation or adhesion. Our SEM and TEM results aligned with the previously published paper, where the authors prepared PLGA nanoparticles by using different drugs³⁴.



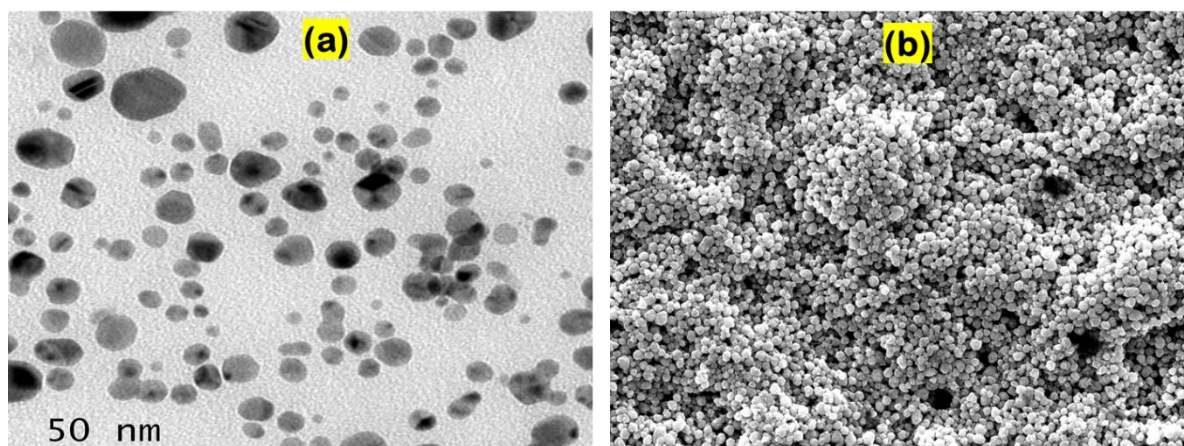


Figure 1. Morphological analysis (a) TEM images of LTZ-PLGA-NPs; (b) SEM images of LTZ-PLGA-NPs(F5)

3.1.2. Particle size, polydispersity index (PDI) and zeta potential

The PDI of LTZ-PLGA-NP is shown in **Figure 2 (a)**. DLS analyzes show that some of the samples were polydispersed (polydispersity index = 0.387) and the reproducibility is fine. Furthermore, the nanoparticles were randomly dispersed across the surface. The stability of the particles is significantly improved and most of the particles are found in the range between 53.19 and nm, which also matches with the particle size detected by the Malvern Zeta sizer. The zeta potential was observed to be -10.9 mV, as shown in **Figure 2 (b)**.

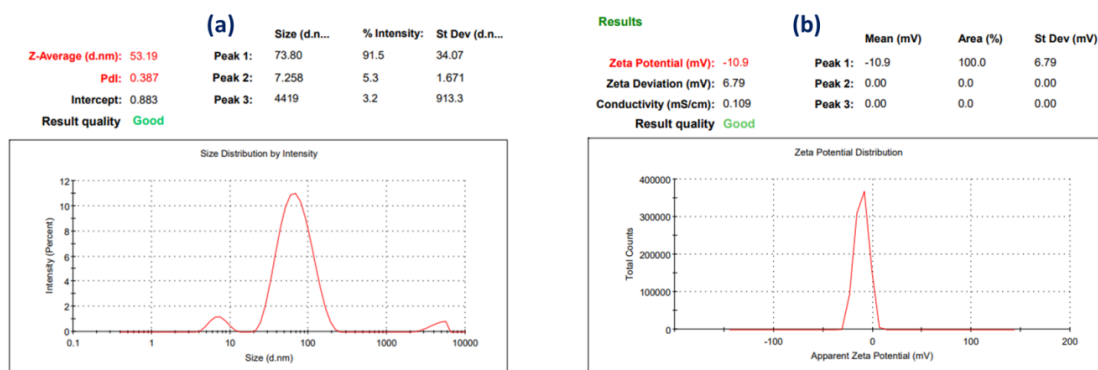


Figure 2. (a) DLS illustrating the size distribution of the particles formed; (b) zeta potential of LTZ-PLGA-NPs(F5)

3.1.3. Drug entrapment efficiency

The encapsulation of drug molecules was carried out by UV-visible spectroscopy, and the results showed the effectiveness of encapsulation. The entrapment efficiency achieved with the final formulation was **76.8%**. The drug entrapment efficiency was very good and our result is in line with the previously published report by Sun et al., where they reported a high encapsulation efficiency of **88.4%**³⁵.

Formulation code	Drug Concentration (mg)	PLGA Concentration (mg)	PVA concentration w/v (%)	Encapsulation (%)
F1	20	10	0.90	26.5±0.59
F2	20	15	0.85	32.6±0.63
F3	20	20	0.80	22.7± 2.19



F4	20	25	0.75	43.67±2.04
F5	20	30	0.70	76.4±3.71

Table 1. Composition of formulation parameters. Values are expressed as Mean ± SEM for 3 samples.

3.1.4. In vitro drug release

Based on drug-encapsulation, we selected formulation code F5 for in vitro drug release study. In vitro release of the drug was carried out for forty-eight hours. In this case, the dialysis bag technique was used to measure the amount of LTZ released by LTZ-PLGA-NPs. A biphasic release profile was determined for the prepared formulations (see **Figure 3 and Table 2**). During the first 8 hours of the experiment, LTZ-PLGA nanoparticles were released, which accounted for between 20% and 30% of the total drug. Time-dependent release curves show a long release profile that leads to an initial release at pH 5 and 7.4. The long-term release rate shows drug overdose and provides sufficient time for LTZ-PLGA-NP. The total LTZ release was 85% after 48 hours. As shown in **Figure 3**, the percentage of LTZ released for more than 42 hours was almost 85.50% at pH 7.4. The sensitivity of LTZ-PLGA-NPs to endosomal pH in the cancer cell environment was 89.5% at pH 5. Consequently, LTZ is released more rapidly at pH 5.0, 37 °C than under physiological conditions (pH 7.4, 37 °C). LTZ was gradually released by two different processes, dissolution and dissemination. The release of the drug from LTZ-PLGA nanoparticles was

expected to be slow due to the strong core at body temperature. Previous studies have also shown that a higher percentage of drug is released from gum acacia stabilized gold nanoparticles (GA-AuNP) under acidic conditions than under neutral conditions³⁶. These results suggest that the LTZ present in PLGA nanoparticles is probably associated with the nanoparticle. The results of the linear regression analysis data are given in **Table 2**. The value of r^2 was found to be high at both pH levels in the Higuchi model with high linearity. Therefore, it is noteworthy that the values r^2 of pH 5.0 (0.9852); and pH 7.0 (0.9909) for the Higuchi model. The Higuchi model implies that the amount of drug release in the dosage form is a function of the square root of time. The highest r^2 value gives an indication that the drug releases. The plots showed that release of a drug involves both pore diffusion and matrix erosion. The drugs in the outer layer exposed to the bath solution are first dissolved and then diffused from the matrix. This process continues with the interface between the bath solution and the solid drug, which moves inward toward the interior. Thus, to control the distribution of this system, the rate of dissolution of drug particles within the matrix must be much faster than the rate of diffusion of dissolved drugs from the matrix³⁷.



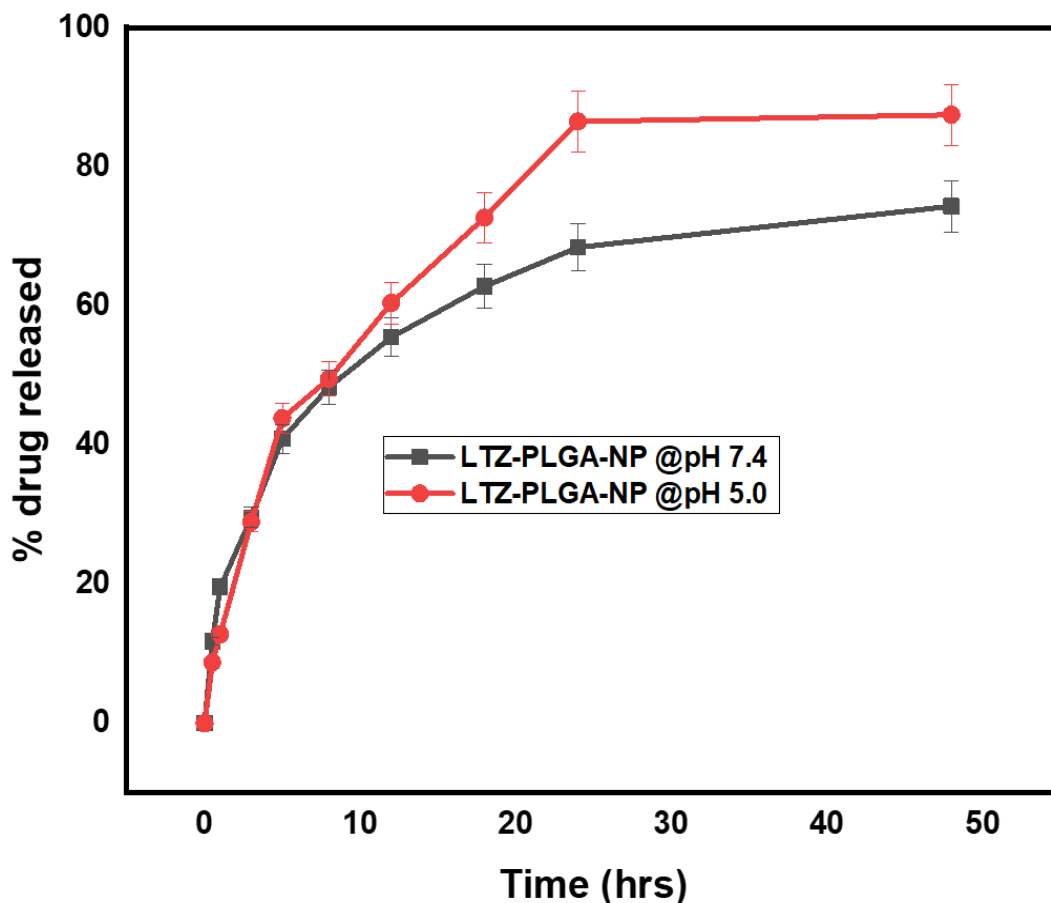


Figure 3. Comparative in vitro cumulative percentage drug release study of LTZ released from LTZ-PLGA-NP(F5)@pH 7.4 and pH 5.0 for 48 hrs. Values are expressed as Mean ± SEM for 3 samples.

Model name	pH 5.0	pH 7.0
Zero-order model	0.9112	0.8763
Higuchi model	0.9852	0.9909
First order	0.9633	0.9388
Korsmeyer-Peppas model	0.9178	0.8712
Hixson-Crowell model	0.9481	0.9199

Table 2: Drug release kinetic model at pH 5.0 & pH 7.0(F5).

3.1.5. In vitro hemolysis assay

The hemolytic toxicity of LTZ-PLGA-NP was studied in relation to erythrocytes suspension (2% hemocrit). Triton X 100 was used as standard hemolytic agent (1% v/v), and the absorption value of Triton X 100 should represent complete hemolysis (100%)³⁸. Triton is a nonionic surfactant that ruptures the RBC membrane and releases hemoglobin. **Figure 4** shows the results of studies investigating the effects of prepared nanoparticles on hemolysis at different concentrations (2-20 µg/ml). PLGA-NPs showed very low hemolysis (2%). The hemolytic effect of LTZ-PLGA -NP in concentrates, i.e., 2, 5, 10, 15, and 20 µg/mL, was inconsistent at intervals below 20%. In addition, LTZ-PLGA-NP has



biocompatible interactions and nontoxic properties. They are considered to be the main means of drug delivery. The above studies on erythrocytes show that the LTZ-PLGA NPs, which make up the LTZ-PLGA NPs in the current research, have potential for biological interactions and can be used safely in the body.

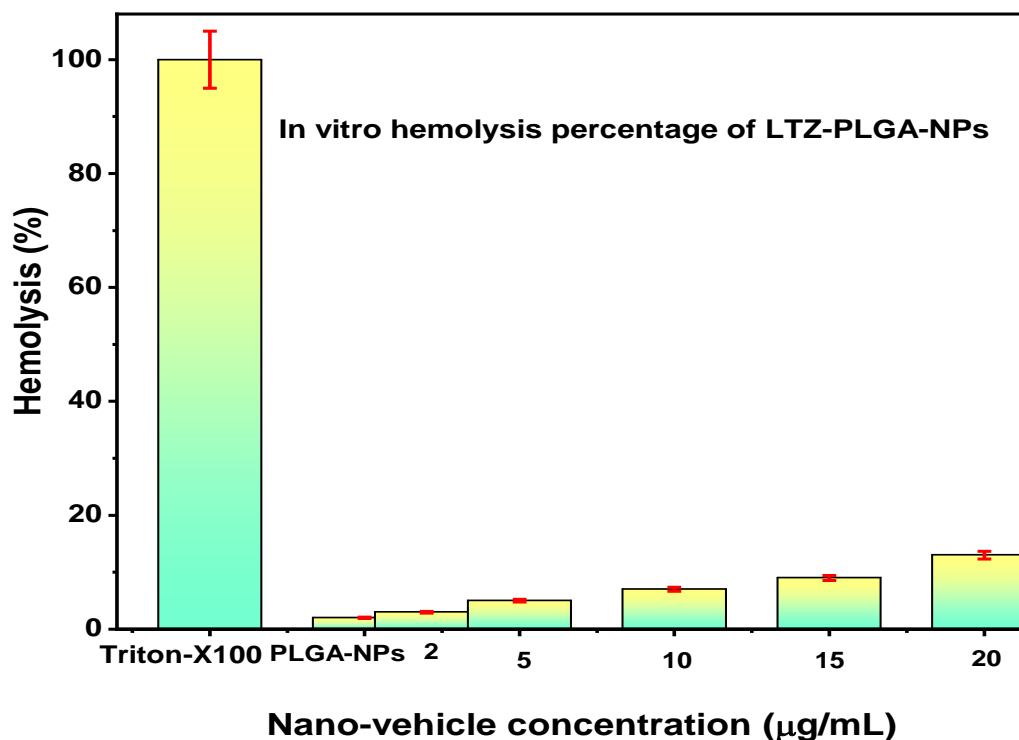


Figure 4. *In vitro* hemolysis percentage of LTZ-PLGA-NPs(F5). Values are expressed as Mean \pm SEM for 3 samples.

3.1.6. Cytotoxicity assay

The results of the MTT assay, which measures cell function, provide a clear description of the mechanisms by which cells respond to the structure of the MDA-MB -231 cell, as shown in **Figure 5**. To determine the effect of LTZ on cell proliferation, the MDA-MB -231 cell line was treated with different LTZ formulations. The results show that LTZ therapy suppresses cell proliferation in cells. In MDA-MB 231 cells, cell growth decreases after LTZ treatment, accompanied by an increase in the percentage of inhibition and a decrease in proliferation percentage after LTZ treatment. The formulation exhibited the highest cytotoxicities for cancerous cells. The probable reason for this is a surface interaction between the LTZ molecule and PLGA, which has stronger binding to the negatively occupied cell membrane. The results of LTZ MTT assay showed that the cytotoxicity increased significantly for MDA-MB -231 cells, which could also be supported by the lower IC50 value of the formula compared to free LTZ. The IC50 value of LTZ-PLGA -NPs 5.64 ± 0.346 $\mu\text{g/ml}$.



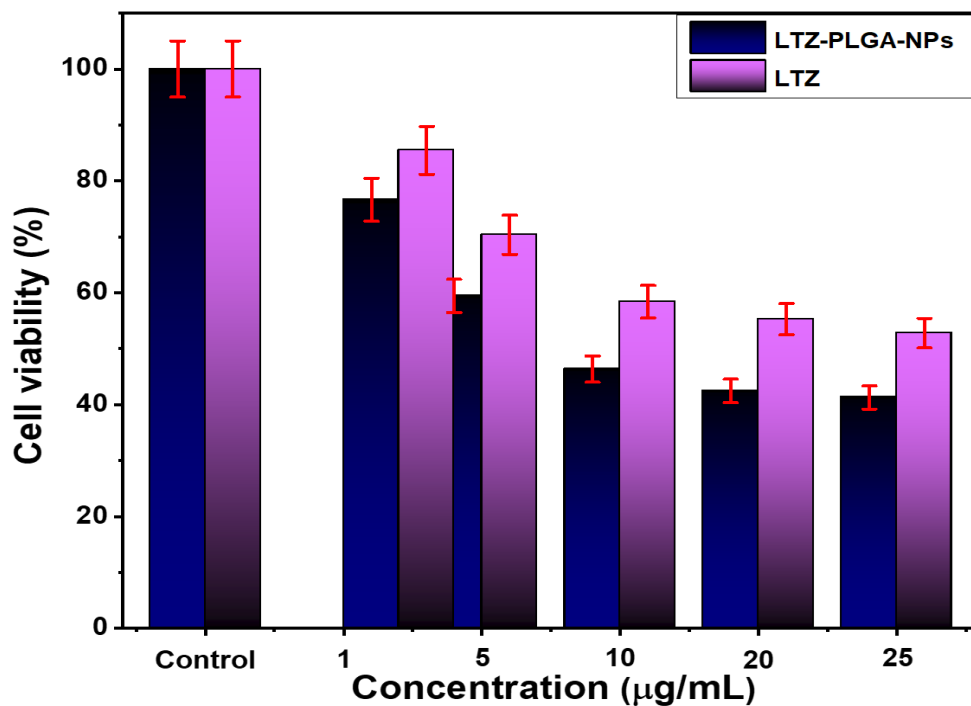


Figure.5 In vitro cytotoxicity and percent cell viability assay against MDA-MB-231 breast cancer cell lines for formulation (F5). Values are expressed as Mean ± SEM for 3 samples.

3.1.7. Stability During Storage

The physical stability of LTZ-PLGA-NP was evaluated by storing samples at room temperature for 30 days. The size, encapsulation efficiency, PDI, and zeta potential of the particles were found to be insignificant, as shown in **Table 3**. On the basis of the stability studies, it can be concluded that the newly constructed structure is stable and suitable for breast cancer treatment.

Room temperature				
Days	Size	PDI	ZP (mV)	EE%
0	53±2.65	0.387±0.01	-10.9±0.54	76.8±3.84
15	56.04±2.80	0.32±0.016	-12.07±0.60	72.3±3.61
30	58.09±2.90	0.367±0.018	-13.2±0.66	67.0±3.39

Table 3: Effect of storage capacity on LTZ-PLGA-NPs (F5) at room temperature. Values are expressed as Mean ± SEM for 3 samples.

4. CONCLUSION

The clinical success of LTZ, a popular anticancer drug, is severely hampered by its nonspecificity and severe dose-limiting toxicities. The aim of this study was to improve LTZ-PLGA NPs and enhance the activity of LTZ by increasing its sustainability in the treatment of breast cancer. In summary, LTZ-loaded PLGA NPs were prepared using a modified version of an oil-in-water

(O/W) single-emulsion solvent evaporation process. The final formation of LTZ-loaded nanoparticles was confirmed by size, shape, encapsulation efficiency, in vitro release studies, and the MTT assay against breast cancer cell lines. The LTZ-loaded PLGA-NP provides a unique formulation approach for sustained drug release with better efficacy against MDA-MB - 231 breast cancer cell lines. In summary, these results



emphasize that LTZ-PLGA NPs exhibit anticancer efficacy against MDA-MB -231 cancer cells.

5. ACKNOWLEDGEMENTS

Ms. Sandhya Rani Mandadi extends her sincere thanks to Indian Council of Medical Research (ICMR), the Government of India, forward of Senior Research Fellowship (SRF). File No. (3/22/17/2019/NCD-III).

6. CONFLICT OF INTEREST

There are no conflicts of interest.

7. FUNDING

Funded by the Indian Council for Medical Research (ICMR), the Government of India, Senior Research Fellowship (SRF). File No. (3/2/2/17/2019/NCD-III).

8. ETHICS APPROVAL

All studies are done in accordance with guidelines of the institutional Animal Ethics Committee, VIPER, Narsapur, Hyderabad, under approval number (01/IAEC/VIPER/Ph.D/2021-2022).

9. REFERENCES

1. Donepudi MS, Kondapalli K, Amos SJ, Venkanteshan P. Breast cancer statistics and markers. *J. Cancer Res. Ther.* 2014;10(3):506.
2. Lavanya S, Santha NJ, Sethu G. A descriptive study to assess the level of stress among women with selected type of cancer in Erode Cancer Centre at Erode. *Asian J Pf Nurs Educ Res.* 2014;4(3):321-324.
3. Bray F, Ferlay J, Soerjomataram I, Siegel RL, Torre LA, Jemal A. Global cancer statistics 2018: GLOBOCAN estimates of incidence and mortality worldwide for 36 cancers in 185 countries. *CA: Cancer J Clin.* 2018;68(6):394-424.
4. Islami F, Torre LA, Drope JM, Ward EM, Jemal A. Global cancer in women: cancer control priorities. *Cancer Epidemiol Biomarkers Prev.* 2017;26(4):458-70.
5. Geetha M, Menaka K, Padmavathi P. Awareness of Breast self-examination and risk factors of Breast Cancer among Women. *Asian J Nurs Educ Res.* 2017;7(3):413-6.
6. Singh S, Numan A, Maddiboyina B, Arora S, Riadi Y, Md S, Alhakamy NA, Kesharwani P. The emerging role of immune checkpoint inhibitors in the treatment of triple-negative breast cancer. *Drug Discov Today.* 2021;26(7):1721-7.
7. Aldawsari HM, Singh S. Rapid microwave-assisted cisplatin-loaded solid lipid nanoparticles: synthesis, characterization and anticancer study. *Nanomaterials.* 2020;10(3):510.
8. Gao L, Zhang D, Chen M. Drug nanocrystals for the formulation of poorly soluble drugs and its application as a potential drug delivery system. *J Nanopart Res.* 2008;10(5):845-62.
9. Santa-Maria CA, Camp M, Cimino-Mathews A, Harvey S, Wright J, Stearns V. Neoadjuvant therapy for early-stage breast cancer: current practice, controversies, and future directions. *Oncology (Williston Park).* 2015;29(11):828.
10. Fedorenko IV, Wargo JA, Flaherty KT, Messina JL, Smalley KS. BRAF inhibition generates a host-tumor niche that mediates therapeutic escape. *J Invest Dermatol.* 2015;135(12):3115-24.
11. Hemalatha CN, Kumar YP, Anandhi VM. Formulation and Characterization of Nanoparticles Loaded with Cefadroxil. *Res J Pharm Technol.* 2017;10(1):183.
12. Peer D, Karp JM, Hong S, Farokhzad OC, Margalit R, Langer R. Nanocarriers as an emerging platform for cancer therapy. *Nat. Nanotechnol.* 2007;2(12):751-60.
13. Jayandran M, Haneefa MM, Balasubramanian V. Synthesis, Characterization and antimicrobial activities of turmeric curcumin and curcumin stabilized zinc nanoparticles-A green approach. *Res J Pharm Technol.* 2015;8(4):445.
14. Mohanty S, Panda S, Purohit D, Si SC. A Comprehensive Review on PLGA-Based Nanoparticles Used for Rheumatoid Arthritis. *Res J Pharm Technol.* 2019;12(3):1481-8.
15. Singh S, Numan A, Cinti S. Point-of-care for evaluating antimicrobial resistance through the adoption of functional materials. *Anal Chem.* 2021; 94(1) 26-40
16. Kumar DV, Verma PR. Development of a poly (ϵ Caprolactone) based nanoparticles for oral delivery of Quercetin. *Res J Pharm Technol.* 2015;8(7):836-40.
17. Manimaran T, Sudhakar T, Nanda A, Bhat MA, Varghese A. Biosynthesis of Green Nanoparticles from *Occimum sanctum* and their Characterization. *Res J Pharm Technol.* 2016;1:3432.
18. Kesharwani P, Iyer AK. Recent advances in dendrimer-based nanovectors for tumor-targeted drug and gene delivery. *Drug Discov Today.* 2015;20(5):536-47.



19. Numan A, Singh S, Zhan Y, Li L, Khalid M, Rilla K, Ranjan S, Cinti S. Advanced nanoengineered—customized point-of-care tools for prostate-specific antigen. *Microchim Acta*. 2022;189(1):1-7.
20. Fatemi HM, Al-Turki HA, Papanikolaou EG, Kosmas L, De Sutter P, Devroey P. Successful treatment of an aggressive recurrent post-menopausal endometriosis with an aromatase inhibitor. *Reprod Biomed online*. 2005;11(4):455-7.
21. Dey SK, Mandal B, Bhowmik M, Ghosh LK, Development and in vitro evaluation of Letrozole loaded biodegradable nanoparticles for breast cancer therapy. *Braz. J. Pharm. Sci.* 2009;45(3):585-91.
22. Kumar SS, Gopalakrishnan G, Gowrishankar NL. Design, Optimization and in vitro Characterization of Dasatinib loaded PLGA Nano carrier for Targeted cancer therapy: A Preliminary Evaluation. *Res J Pharm Technol*. 2021;14(4):2095-100.
23. Singh S, Numan A, Zhan Y, Singh V, Van Hung T, Nam ND. A novel highly efficient and ultrasensitive electrochemical detection of toxic mercury (II) ions in canned tuna fish and tap water based on a copper metal-organic framework. *J Hazard Mater*. 2020; 15;399:123042.
24. Singh S, Alrobaian MM, Molugulu N, Agrawal N, Numan A, Kesharwani P. Pyramid-shaped PEG-PCL-PEG polymeric-based model systems for site-specific drug delivery of vancomycin with enhance antibacterial efficacy. *ACS Omega*. 2020; 5(21):11935-45.
25. Numan A, Gill AA, Rafique S, Guduri M, Zhan Y, Maddiboyina B, Li L, Singh S, Dang NN. Rationally engineered nanosensors: A novel strategy for the detection of heavy metal ions in the environment. *J Hazard Mater*. 2021;409:124493.
26. Singh S, Numan A, Zhan Y, Singh V, Alam A, Van Hung T, Nam ND. Low-potential immunosensor-based detection of the vascular growth factor 165 (VEGF 165) using the nanocomposite platform of cobalt metal-organic framework. *RSC Adv*. 2020;10(46):27288-96.
27. Gad SC, editor. *Drug discovery handbook*. John Wiley & Sons; 2005 Jun 24.
28. Singh S, Vardhan H, Kotla NG, Maddiboyina B, Sharma D, Webster TJ. The role of surfactants in the formulation of elastic liposomal gels containing a synthetic opioid analgesic. *Int J Nanomedicine*. 2016;11:1475.
29. Chapdelaine JM. MTT reduction—a tetrazolium-based colorimetric assay for cell survival and proliferation. *Pharm Res Int*; 2010. 2001:1-6.
30. Arabsolghar R, Saberzadeh J, Khodaei F, Borojeni RA, Khorsand M, Rashedinia M. The protective effect of sodium benzoate on aluminum toxicity in PC12 cell line. *Res Pharm Sci*. 2017;12(5):391
31. Li Y, He H, Jia X, Lu WL, Lou J, Wei Y. A dual-targeting nanocarrier based on poly (amidoamine) dendrimers conjugated with transferrin and tamoxifen for treating brain gliomas. *Biomaterials*. 2012;33(15):3899-908.
32. Khagga B, Kaitha MV, Dammu R, Mogili S. ICH guidelines—“Q” series (quality guidelines)—A review. *GSC Biol Pharm Sci*. 2019;6(3):089-106.
33. Bajaj S, Singla D, Sakhuja N. Stability testing of pharmaceutical products. *J Appl Pharm Sci*. 2012;2(3):129-38.
34. Betancourt T, Brown B, Brannon-Peppas L. Doxorubicin-loaded PLGA nanoparticles by nanoprecipitation: preparation, characterization and in vitro evaluation. *Nanomedicine (Lond)*. 2007 Apr;2(2):219-32.
35. Sun SB, Liu P, Shao FM, Miao QL. Formulation and evaluation of PLGA nanoparticles loaded capecitabine for prostate cancer. *Int J Clin Exp Med*. 2015 Oct 15;8(10):19670-81.
36. Aldawsari HM, Singh S, Alhakamy NA, Bakhaidar RB, Halwani AA, Badr-Eldin SM. Gum Acacia Functionalized Colloidal Gold Nanoparticles of Letrozole as Biocompatible Drug Delivery Carrier for Treatment of Breast Cancer. *Pharmaceutics*. 2021 Sep 24;13(10):1554.
37. Jaimini M, Kothari AH. Sustained release matrix type drug delivery system: A review. *Journal of drug delivery and therapeutics*. 2012 Nov 15;2(6).
38. Ganesan, S., Chaurasiya, N.D., Sahu, R., Walker, L.A. and Tekwani, B.L., 2012. Understanding the mechanisms for metabolism-linked hemolytic toxicity of primaquine against glucose 6-phosphate dehydrogenase deficient human erythrocytes: evaluation of eryptotic pathway. *Toxicology*, 294;54-60.

